DUPLICATE ALSO

Forecasting Research

Forecasting Research Division
Scientific Paper No. 29

NEW SHALLOW FLOWS OVER AN OBSTACLE

by

A.S. Broad , D. Porter and M. J. Sewell

19 October 1994

Meteorological Office
London Road
Bracknell
Berkshire
RG12 2SZ
United Kingdom

ORGS UKMO F
National Meteorological Library
FitzRoy Road, Exeter, Devon. EX1 3PB

Forecasting Research Division
Scientific Paper No. 29

NEW SHALLOW FLOWS OVER AN OBSTACLE

by

A.S. Broad , D. Porter and M. J. Sewell

19 October 1994

NEW SHALLOW FLOWS OVER AN OBSTACLE

by

A.S. Broad*, D. Porter† and M.J. Sewell*†

*Meteorological Office, Bracknell,

and

†Department of Mathematics, University of Reading

19 October 1994

Abstract

Lowest order shallow water theory is applied to flow, in a single vertical plane, over a wide class of monotonic mountains. Many new flows are described. These include steady continuous smoothly bifurcating flows, in which the fluid speed and the free surface profile bifurcate smoothly at the apex of the mountain, unless the mountain is locally parabolic there. In the latter case the free surface bifurcation is known to be abrupt and not smooth at the apex, but we show that this is the exception. We demonstrate that the fluid speed and free surface shape are sensitive to the mountain shape near the apex. Pseudo–steady flows, containing a bore travelling upstream away from the obstacle, are exhibited. In some cases the bore relieves what would otherwise be a blocked continuous flow. If the incoming Froude number is not too large, the bore can lift the fluid so that it subsequently flows over the obstacle either freely or, if energy dissipation is minimized at the bore, with a bifurcation at the apex. Such bores can also coexist with what would otherwise be a bifurcating or a free continuous flow. The strength ranges which are admissible for all these bores are determined. A complete geometrical representation of all the possible bores is given, in a three dimensional parameter space for the first time.

© Crown Copyright 1994.

1. Introduction

There is a large literature about flows over obstacles, under diverse hypotheses, for example either with or without stratification, either with or without a shallow water theory to some order of approximation, and allowing for either one or two horizontal dimensions. This paper describes many new results for the simplest of these theories.

We study the flow of homogeneous incompressible inviscid fluid, in a single vertical plane, under the hypotheses of lowest order shallow water theory, over an obstacle having monotonic sides rising to a single apex from both directions. A much larger family of such "monotonic mountains" than previously considered is included. The most familiar obstacle in the literature is the parabolic one, and we show that details of flow over this are not representative of flows over members of the larger family.

We build upon previous work by Long (1954, 1970, 1972), Houghton and Kasahara (1968), Baines et al. (1980, 1984, 1987), Pratt (1983, 1984) and Lawrence (1987). This paper includes, in particular, a concise account of some results from a more wide–ranging study by Broad, Porter and Sewell (1992a, b), and provides significant extensions of these results.

In §3 we define the obstacle profiles. We exhibit steady continuous free flows over them. We also specify conditions under which the free surface and the fluid speed bifurcate at the apex. A new result, as far as we are aware, is that the bifurcation is smooth unless the profile is parabolic, the latter being the only case in which the bifurcation is abrupt. Pratt (1984) gives the most explicit previous recognition of an abrupt bifurcation over a parabolic apex.

When the apex is so high that it blocks continuous flow, we show in §§5 and 6 how this blocking can be relieved by a bore travelling upstream from the obstacle. The bore raises the free surface so that it passes over the apex either freely, or with a bifurcation there, depending on whether or not more than a minimum energy is dissipated at the bore.

We also prove, for the first time, that there is a maximum supercritical incoming Froude number above which blocking cannot be relieved by such bores. In §5 we also give a number of new solutions, including specific ranges of bore strength, in which bores can occur in an already free or bifurcating flow.

In §7 we summarize our results, and we express them all geometrically in a three dimensional parameter space spanned by incoming Froude number, mountain apex height, and bore strength. This is a significant extension of the so–called classification diagrams which have previously appeared in the literature, as we indicate in §8.

2. Flow Variables

We define notation as follows. x is the horizontal coordinate. $b(x)$ is a given continuous function whose values are the height of the bed above a fixed horizontal level. t is time, and $d(x, t) > 0$ is an unknown function whose values are the fluid depth above the bed. $u(x, t) \geq 0$ is an unknown function whose values are the horizontal fluid speed. $Q = ud \geq 0$ is mass flux. $s = d + b$ is free surface height. g represents acceleration due to gravity. $e = \frac{1}{2} u^2 + gs$ is total energy (kinetic + potential + pressure energy) of the representative fluid particle according to lowest order shallow water theory. $F = u/(gd)^{\frac{1}{2}}$ is the Froude number.

Where $u > 0$, i.e. except in still water, these definitions imply that

$$b(x) = \frac{1}{g}(e - \tfrac{1}{2} u^2) - \frac{Q}{u}. \tag{1}$$

We also define

$$G = \frac{2(e-gb)}{3(gQ)^{2/3}}, \quad \text{so that} \quad G = \frac{1}{3}F^{4/3} + \frac{2}{3}F^{-2/3}. \tag{2}$$

The function $G(F)$ in $(2)_2$ is convex with a minimum at $G(1) = 1$, as shown in Figure 1. This proves that where $G < 1$ no flow is possible; that where $G = 1$ one flow (called *critical*, with $F = 1$) is possible; and that where $G > 1$ two flows are possible, one being *subcritical* $(F < 1)$ and the other *supercritical* $(F > 1)$.

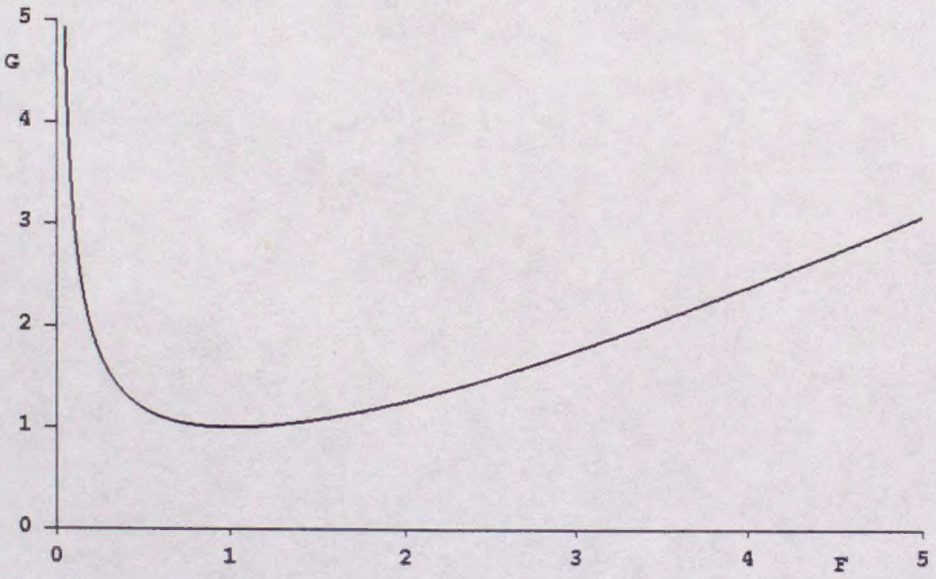

Figure 1 $G = \frac{1}{3}F^{4/3} + \frac{2}{3}F^{-2/3}$

3. Steady Flow over a Monotonic Mountain

Where the flow is steady and continuous the differential equations of mass and horizontal momentum balance require that, for all x and t,

$$Q = \text{constant} \quad \text{and} \quad e = \text{constant} \tag{3}$$

respectively. Assuming this $Q > 0$, the right side of (1) is a concave function of u having a maximum value

$$\frac{1}{g}\left[e-\frac{3}{2}(gQ)^{2/3}\right] = k \text{ (say)} \tag{4}$$

at $u=(gQ)^{1/3}$. If $Q=0$, then $s=$ constant and $k=s$.

We suppose that the given bed function $b(x)$ has a maximum value, say $a>0$, at the apex of the obstacle. Then the flow (3) will be *free* to pass over the obstacle if $a<k$, but it will be *blocked* by the obstacle if $a>k$. We shall demonstrate that the flow can *bifurcate* at the apex if $a=k$, and we call such a flow a *bifurcating* flow.

We define a *monotonic mountain* to be any profile whose $b(x)$ rises monotonically to the apex value a and then falls monotonically away from it. A simple model of a monotonic mountain is

$$b(x) = \begin{cases} a\left[1-\left[\dfrac{\nu-x}{\nu+\ell}\right]^{\sigma}\right] & -\ell \le x \le \nu \\ \\ a\left[1-\left[\dfrac{x-\nu}{\ell-\nu}\right]^{\sigma}\right] & \nu \le x \le \ell \end{cases} \tag{5}$$

with $b(x)=0$ where $|x| \ge \ell$. Here a, ℓ, ν and σ are assigned parameters. We assume $\ell > |\nu|$ and $\sigma > 0$. The apex height $a>0$, but (5) with $a<0$ also models a depression in an otherwise flat bed. The length of the mountain or depression is 2ℓ, and the value of ν/ℓ indicates its asymmetry. The value of $1/\sigma$ is a measure of the sharpness of the apex. Five asymmetric examples of (5), with $\nu=\ell/3$, and one symmetric example with $\nu=0$, are displayed at the bottoms of the individual diagrams in Figure 2, for $\sigma = 1,\ 1.5,\ 2,\ 3,\ 10$ and 2 respectively, and with $a=1.01$ in all six profiles.

Equation (1) shows how u must vary with x in the flow (3). We display three cases of this dependence, for each of the six obstacles just described, in Figure 2. To do this we have chosen the values $Q=9$, $e=7.5$ and $g=1$. These are representative of a trio of Q, e, g values which ensure the existence of a *pair* of incoming or outgoing flows with constant u over the distant flat bed $|x|>\ell$, one subcritical ($F=0.54<1$ with

$u = 1.37$, $d = 6.56$) and one supercritical ($F = 1.73 > 1$ with $u = d = 3$) there. There are various equivalent ways of proving the existence of such a pair. One way is to observe that the chosen trio ensures $G = 1.16 > 1$ where $b = 0$, and hence the existence of the stated pair of incoming flows, by the convexity in Figure 1.

Over the obstacle each member of the pair ceases to have constant u. When $a = k$ ($= 1.01$ for the chosen constants), the two flows (labelled 1.01) are seen to come together at a bifurcation where $F = 1$ over the apex, and the bifurcation is smooth unless $\sigma = 2$, when it is abrupt. The obstacle profiles shown in Figure 2 are also for $a = 1.01$, as stated above. When $a < k$, the two $u(x)$ functions (labelled 0.7, and corresponding to $a = 0.7$) approach each other but do not come together, so they indicate two free flows, one always subcritical and one always supercritical. When $a > k$, the two $u(x)$ functions (labelled 1.2, and corresponding to $a = 1.2$) join up and never reach the apex, thus signifying blocking of each putative flow.

The free surface height functions $s(x)$ are qualitatively the same as the $u(x)$ functions, and look very similar (Broad, Porter and Sewell, 1994), except that the supercritical $s(x)$ surfaces are below the subcritical ones, whereas Figure 2 shows the supercritical $u(x)$ functions to be above the subcritical ones.

The nature of the bifurcations of $s(x)$ and $u(x)$ at the apex when $a = k$ can be explored analytically as follows for any piecewise differentiable function $b(x)$, not merely the example (5). First we deduce that where $b = k$, (2) and (4) imply $G = 1$ and therefore $F = 1$ above the apex. Now suppose that (1) has the piecewise differentiable parametric solution $x = x(\epsilon)$, $u = u(\epsilon)$, which is also regular in the sense that we can subsequently choose the parameter ϵ to be either x or u, depending on the case. Then if a prime denotes one–sided ϵ–differentiation, two differentiations of (1) evaluated at the apex imply

$$\frac{db}{dx}x' = 0 \quad , \quad \frac{d^2b}{dx^2}x'^2 + \frac{db}{dx}x'' = -\frac{3}{g}u'^2 . \tag{6}$$

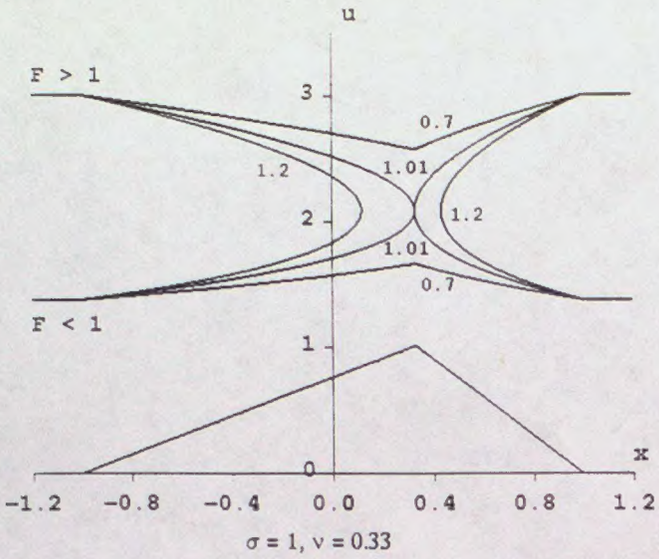

σ = 1, ν = 0.33

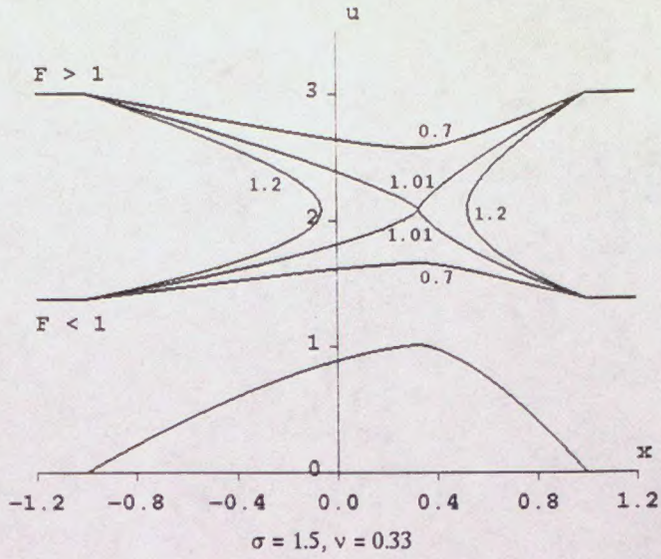

σ = 1.5, ν = 0.33

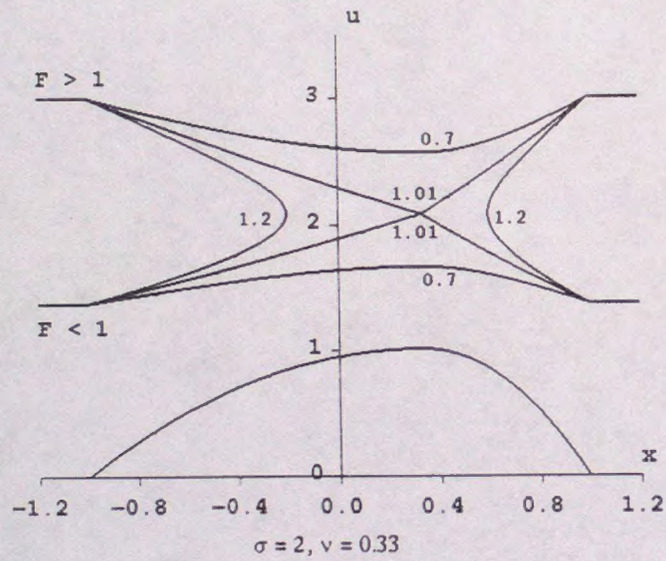

σ = 2, ν = 0.33

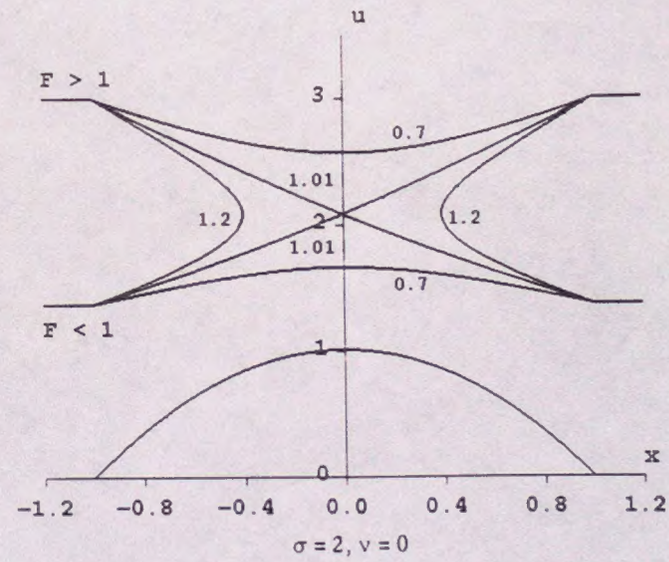

σ = 2, ν = 0

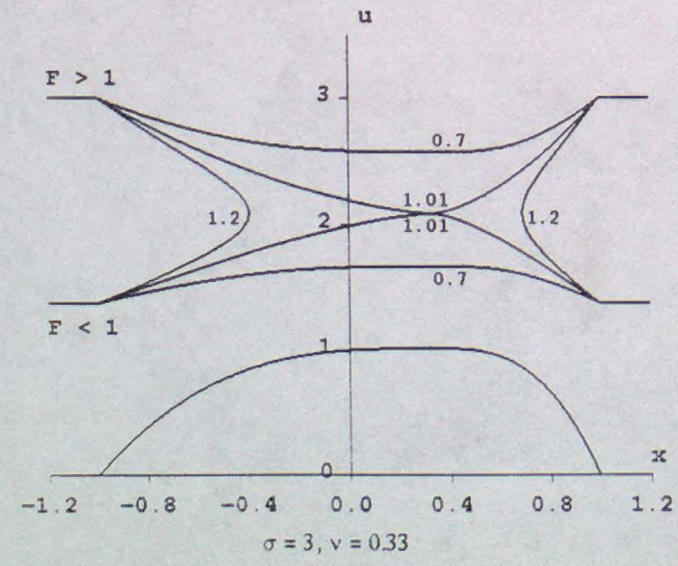

σ = 3, ν = 0.33

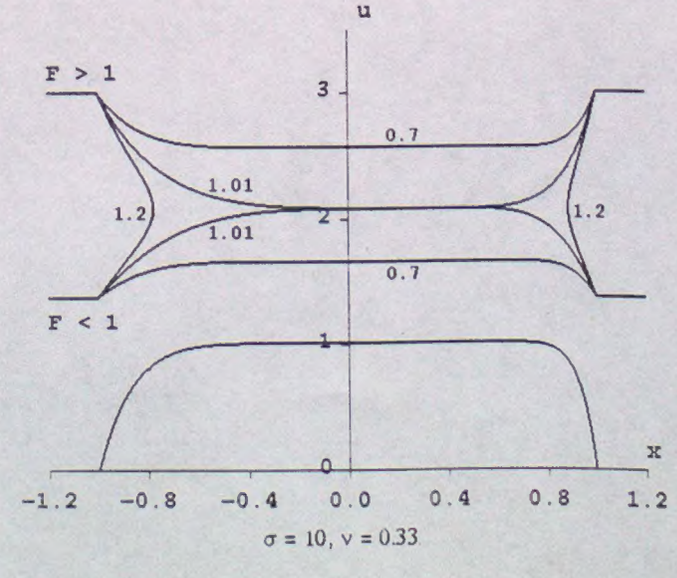

σ = 10, ν = 0.33

Figure 2 Fluid speed functions u(x) over monotonic mountains (5).

For a sharp apex with finite $db/dx \neq 0$, $x' = 0$. We then choose $\epsilon = u$, so that $dx/du = 0$ and $(db/dx)(d^2x/du^2) < 0$ when d^2b/dx^2 is finite. This is consistent with the case $\sigma = 1$ shown in Figure 2.

For a smooth apex $db/dx = 0$. If d^2b/dx^2 is infinite, as it is for (5) when $1 < \sigma < 2$, we can choose $\epsilon = u$ so that $dx/du = 0$, as Figure 2 illustrates for $\sigma = 1.5$.

For a smooth apex with finite d^2b/dx^2, as is true for (5) with $\sigma = 2$, we can choose $\epsilon = x$ so that

$$\frac{du}{dx} = \pm \left[-\frac{g}{3} \frac{d^2b}{dx^2} \right]^{\frac{1}{2}} . \tag{7}$$

This confirms the abrupt bifurcation observed by Pratt (1984) for the case $\sigma = 2$, $\nu = 0$ illustrated in Figure 2. It also describes abrupt bifurcations in which there is a discontinuity in d^2b/dx^2 and therefore du/dx through the apex, as illustrated for $\sigma = 2$, $\nu = \ell/3$ in Figure 2. Furthermore, $d^2b/dx^2 = 0$ implies $du/dx = 0$, as Figure 2 illustrates for $\sigma > 2$, and third or higher differentiations of (1), to supplement (6), will reveal the smooth bifurcations explicitly.

These local considerations do not specify which of the two solutions made available by the bifurcation will be followed when the particle leaves the apex. It might be suggested, in the common case of the symmetric parabolic obstacle ($\sigma = 2$, $\nu = 0$), that (for example) an incoming supercritical flow will choose the subcritical outgoing option in order to preserve smoothness of $u(x)$ (and $s(x)$) at the apex. Such a criterion ceases to be available in the asymmetric case $\sigma = 2$, $\nu \neq 0$, as Figure 2 shows for $\nu = \ell/3$, because both outgoing flows would require a gradient discontinuity. Such a criterion even ceases to be applicable for smoother obstacles with $\sigma > 2$, because the smooth bifurcations show that no transition is abrupt. A thorough further investigation is required of the extra criteria needed to select the outgoing solution. One type of criterion is a stability analysis, such as that of Pratt (1984) for $\sigma = 2$. Another type is the effect of downstream conditions, which we have not needed to specify here. For example, Gill (1977) considers a solution in which there is a stationary bore in the lee of a parabolic obstacle. Analogous

problems in evolving equilibrium states of solids or structures envisage the presence of imperfections to choose between bifurcations of a perfect system.

4. Dynamics of Bores

A bore is a finite discontinuity in d. Here we summarize the dynamical properties of a bore at any location.

Let $C\underline{m}$ be bore velocity, where $\underline{m}$ is a unit vector directed to the right, and C may have either sign. Let $u\underline{m}$ be particle velocity, where u may have either sign at this stage. Then $(u - C)\underline{m}$ is velocity of particle relative to bore. Define $w = u - C$.

At the bore certain quantities, such as d and u, experience a finite jump in their values. We designate values immediately to the right and left of a bore by plus and minus subscripts respectively, and their difference by a square bracket in the sense that $[d] = d_+ - d_-$, for example.

The jump conditions of mass and horizontal momentum balance at the bore are

$$[wd] = 0 \quad \text{and} \quad [w^2 d + \tfrac{1}{2} g d^2] = 0 \tag{8}$$

respectively. The bore has $[d] \neq 0$ with $d_+ > 0$ and $d_- > 0$ by definition. Then (8) implies $w_+ w_- > 0$, so that particles do cross the bore. We can choose this transit to be from left to right without loss of generality, so that $w_+ > 0$ and $w_- > 0$. The hypothesis of energy loss at the bore implies, with (8), that an energy flux quantity

$$E = \tfrac{1}{4} g\,[u]\,[d]^2 < 0 \quad \text{so that} \quad [u] < 0\,. \tag{9}$$

The three physical principles also imply

$$[u] = -[d] g^{\frac{1}{2}} \left[\frac{d_+ + d_-}{2 d_+ d_-}\right]^{\frac{1}{2}} \quad \text{so that} \quad [d] > 0\,, \tag{10}$$

$$C = u_- - \left[\frac{g d_+ (d_+ + d_-)}{2 d_-}\right]^{\frac{1}{2}} \quad \text{and} \quad [e] < C[u]\,. \tag{11}$$

Energy loss also implies that the jump must be such that $w_- > (gd_-)^{\frac{1}{2}}$ and $w_+ < (gd_+)^{\frac{1}{2}}$.

Deem the left side of the bore to be the known side, and the right side to be the unknown side. Then d_- and u_- are known, and we enquire how much information (8) to (11) give about d_+ and u_+, for example in terms of the non–dimensional quantities

$$\lambda = \frac{d_+}{d_-} \quad \text{and} \quad \mu = \frac{\lambda u_+}{(gd_-)^{\frac{1}{2}}}, \quad \text{with} \quad F_- = \frac{u_-}{(gd_-)^{\frac{1}{2}}}. \tag{12}$$

Conditions (9), $(10)_1$ and $(11)_1$ imply

$$E = -g^{3/2}\left[\frac{d_-}{2}\right]^{5/2}(\lambda-1)^3\left[\frac{\lambda+1}{\lambda}\right]^{\frac{1}{2}}, \tag{13}$$

$$\mu = \lambda F_- - (\lambda-1)\left[\tfrac{1}{2}\lambda(\lambda+1)\right]^{\frac{1}{2}}, \tag{14}$$

$$\frac{C}{(gd_-)^{\frac{1}{2}}} = F_- - \left[\tfrac{1}{2}\lambda(\lambda+1)\right]^{\frac{1}{2}}. \tag{15}$$

The domain of interest of (13) – (15) is $\lambda > 1$, by (10). Their range is calculable and depends upon F_-. We call λ the *bore strength.*

In subsequent Sections we confine attention to $u_- > 0$, so that F_- is the incoming Froude number at the bore.

Here we note that if still water is on the left of the bore ($u_- = 0$), the bore must be moving to the left ($C < 0$), and sets particles in motion which move to the left more slowly than itself ($0 < -u_+ < -C$).

In the absence of other considerations (such as the presence of an obstacle somewhere in the flow), any strength value $\lambda > 1$ can be inserted into (14) – (15) to define the bore.

5. Analysis of Bores

In the remainder of the paper we determine the conditions which allow a bore satisfying

$$u_- > u_+ > 0 \geq C \quad , \quad k_+ \geq a \tag{16}$$

to be the transition from one steady flow to another, with the bore located on the flat plain upstream (to the left) of an obstacle of any shape (not necessarily (5)) and apex height a. Such a bore is either stationary ($C = 0$), or moving away from the obstacle ($C < 0$). We exclude $C > 0$, because such a bore would run up against the obstacle. The bore must face upstream, by $(10)_2$. Although it slows the fluid down, as $(9)_2$ requires, we confine attention to the case in which the bore does not stop or reverse the fluid. The outgoing flow will pass over the obstacle either freely (if $k_+ > a$) or with a bifurcation at the apex (if $k_+ = a$).

The overall flow is steady if $C = 0$, but *pseudo–steady* if $C < 0$, in the sense that it is steady everywhere except at the location through which the bore is currently passing.

The incoming flow may be either blocked (if $k_- < a$), bifurcating at the apex (if $k_- = a$) or free (if $k_- > a$). Although the relief of such blocking by a bore satisfying (16) is the initial motivation for our study, the analysis of such a bore in a bifurcating or free incoming flow requires the same mathematical functions, to be described in this Section, and so can be treated economically at the same time.

The analysis turns out to be controlled by the juxtaposition, for each incoming F_-, of the three functions $\lambda^{3/2}$, $\mu(\lambda)$ in (14), and $k_+(\lambda)$ defined by

$$\frac{k_+}{d_-} = \frac{1}{2}\left[\frac{\mu}{\lambda}\right]^2 + \lambda - \frac{3}{2}\mu^{2/3} \tag{17}$$

from (4) at $b = 0$, (12) and (14). To explore the mathematical properties of these functions it is convenient to work first on the domain $\lambda \geq 0$, which is bigger than the

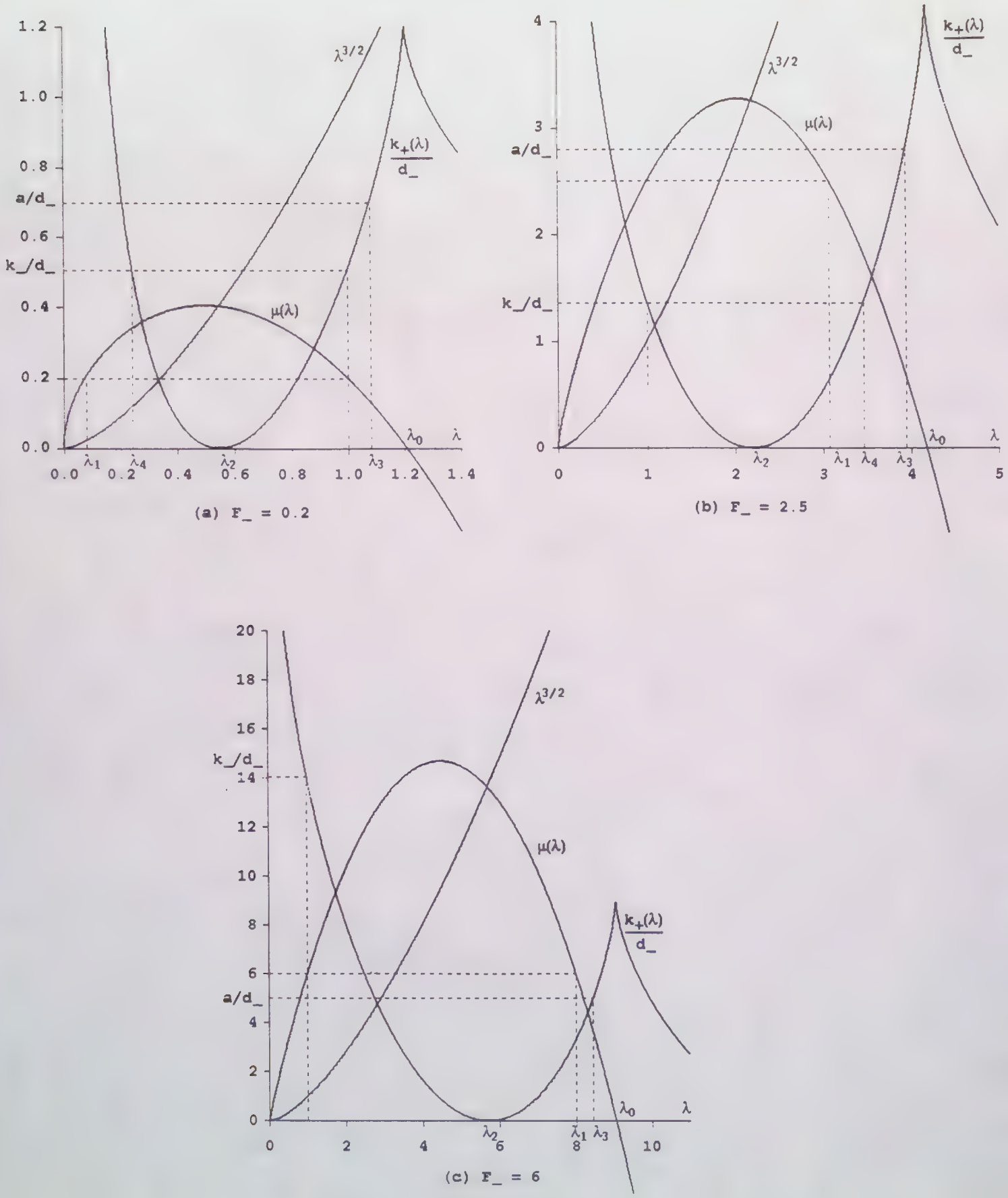

Figure 3. Examples of $\mu(\lambda)$ and $k_{-}(\lambda)$ and their juxtaposition with $+\lambda^{3/2}$.

domain $\lambda > 1$ of eventual physical interest specified by $(10)_2$. To appreciate the following general properties it will be helpful to refer to the particular curves shown in Figure 3 for subcritical $F_- = 0.2$, supercritical $F_- = 2.5$, and hypercritical $F_- = 6$. In Theorem 2(i) we shall give reasons why an inflow with $F_- \geq 4.47$ may conveniently be called "hypercritical".

The function $\mu(\lambda)$ is strictly concave for each given F_-. It has a single stationary maximum at λ_m, say, and λ_m increases with F_-, having $\lambda_m = 1$ at $F_- = 1$. Clearly $\mu(0) = 0$, and there is a single positive value λ_0, say, where $\mu(\lambda_0) = 0$. The domain $0 \leq \lambda \leq \lambda_0$ illustrated in Figure 3 is then sufficient to discuss flows which do not reverse at the bore, because $\mu \geq 0$ there. It can be proved from the properties of cubics that

$$\lambda_0 = \tfrac{1}{3}\left[1 + 2(4 + 6F_-^2)^{\frac{1}{2}}\cos\tfrac{1}{3}\psi\right] \tag{18}$$

where

$$\cos\psi = (9F_-^2 - 8)(4 + 6F_-^2)^{-3/2} \quad \text{and} \quad 0 \leq \psi \leq \pi .$$

This function $\lambda_0(F_-)$ in (18) is shown in each part of Figure 4. No bore which does not reverse the flow can have strength greater than λ_0.

A sufficient range of physical interest for $\mu(\lambda)$ is $0 < \mu < F_-$, because $u_+ > 0$ and $\lambda > 0$ imply $\mu > 0$, and $(8)_1$ with (16) implies $[Q] = C[d] \leq 0$, so that $Q_+ \leq Q_-$ and therefore $\mu \leq F_-$. From (14) either $\mu(1) = F_-$ or $\mu(\lambda_1) = F_-$, thus defining a function $\lambda_1(F_-)$ by

$$\lambda_1 = \tfrac{1}{2}\left[(1 + 8F_-^2)^{\frac{1}{2}} - 1\right], \tag{19}$$

which increases as shown in Figure 4. A sufficient domain of physical interest for λ is therefore $1 \leq \lambda < \lambda_0$ if $F_- \leq 1$, and $\lambda_1 \leq \lambda < \lambda_0$ if $F_- \geq 1$, and $\mu(\lambda)$ is a monotonically decreasing function on both domains, as illustrated in Figure 3. Bores with strength λ_1 are stationary, and stronger bores move to the left. We can reduce these λ domains even more by arguments which follow in Theorem 2.

The function $+\lambda^{3/2}$ is strictly convex with zero slope at $\lambda = 0$.

Let λ_2 denote the unique intersection of $+\lambda^{3/2}$ and $\mu(\lambda)$ for each F_-. It follows from (17) that $k_+(\lambda)$ has a stationary zero at λ_2, so that $k_+(\lambda_2) = 0$. Allowing F_- to vary in this equation defines the function $\lambda_2(F_-)$ shown in Figure 4. For each F_- the function $k_+(\lambda)$ is convex in $0 < \lambda \le \lambda_0$ and monotonically increasing in $\lambda_2 \le \lambda \le \lambda_0$. Clearly $k_+(\lambda_0) = \lambda_0 d_-$, and $k_+(\lambda)$ has a cusped local maximum at this point as shown in Figure 3, before falling to another zero minimum and then rising to infinity. We mention this cusp in passing, because any investigation of bores which reverse the flow ($\mu < 0$) will need to use it. We need λ_2 to prove Theorem 1(i) below. Figure 4 shows that $\lambda_2(F_-)$ and $\lambda_1(F_-)$ cross over at $F_- = 1$, with $\lambda_1 > \lambda_2$ for $F_- > 1$.

Let λ_3 be the particular bore strength satisfying $k_+(\lambda_3) = a$, i.e. such that the outgoing flow bifurcates at the apex. The monotonically increasing property of $k_+(\lambda)$ in $\lambda_2 \le \lambda \le \lambda_0$ for each F_- shows that λ_3 is unique there for each $a \le \lambda_0 d_-$. Examples are indicated in Figure 3 for the values $a/d_- = 0.7, 2.8, 5$ when $F_- = 0.2, 2.5, 6$ respectively. Allowing F_- to vary permits $k_+(\lambda_3) = a$ to be written more explicitly, in terms of the function $\mu(\lambda, F_-)$ in (14) and (17), as

$$\frac{a}{d_-} = \frac{1}{2}\left[\frac{\mu(\lambda_3,\ F_-)}{\lambda_3}\right]^2 + \lambda_3 - \frac{3}{2}\left[\mu(\lambda_3, F_-)\right]^{2/3}. \qquad (20)$$

The parameter a/d_- is apex height normalized by incoming fluid depth.
This equation implicitly defines a function $\lambda_3(F_-, a/d_-)$, and therefore a function $\lambda_3(F_-)$ for each choice of a/d_-. The latter function is obtained numerically and illustrated in Figure 4 for $\lambda_3 \le \lambda_0$, which is sufficient for our purpose, for the values $a/d_- = 0.4, 1.5, 4$ and 8. The increasing property of $k_+(\lambda)$ shows that no bore of strength less than λ_3 will satisfy (16), because the outflow from it would be blocked ($k_+ < a$). As $a/d_- \longrightarrow 0$, $\lambda_3(F_-) \longrightarrow \lambda_2(F_-)$.

From the fact that (4) can be written alternatively as

$$\frac{k - b}{d} = \frac{1}{2}F^2 + 1 - \frac{3}{2}F^{2/3} \qquad (21)$$

we can see that, where $b = 0$,

$$\frac{k_-}{d_-} = \frac{1}{2}F_-^{\,2} + 1 - \frac{3}{2}F_-^{\,2/3}. \tag{22}$$

This function is shown in Figure 4, and it intersects $\lambda_0(F_-)$ where $F_- = 4.47$ and $\lambda_0 = 6.90$. If $\lambda = 1$, $\mu = F_-$ and therefore $k_+(1) = k_-$ from (14), (17) and (22).

Let $\lambda_4 \leq \lambda_0 \leq 6.90$ denote the second root of $k_+(\lambda_4) = k_-$ which Figure 3 illustrates when $F_- \leq 4.47$. More explicitly,

$$\frac{1}{2}F_-^{\,2} + 1 - \frac{3}{2}F_-^{\,3/2} = \frac{1}{2}\left[\frac{\mu(\lambda_4, F_-)}{\lambda_4}\right]^2 + \lambda_4 - \frac{3}{2}\left[\mu(\lambda_4, F_-)\right]^{2/3} \tag{23}$$

defines a function $\lambda_4(F_-)$ which is shown in Figure 4 within $1 \leq F_- \leq 4.47$ by solving (23) numerically. Its end points there are $\lambda_4(1) = 1$ and $\lambda_4(4.47) = 6.90$. If a bore of strength λ_4 could exist it would not change the value of k in (4), and therefore it would not change the propensity of the incoming flow to surmount the obstacle.

The particular values α, β and γ of F_- which are shown in Figure 4 are defined as follows.

If $0 < a/d_- < 1$ there are two values $\alpha < 1$ and $\beta > 1$ of F_- such that $a = k_-$ (thus defining inflows which would bifurcate over the apex). If $a = 0$, $\alpha = \beta = 1$. If $a = d_-$, $\alpha = 0$ and $\beta = 2.28$. If $1 \leq a/d_- \leq 6.90$, β is defined in the same way and satisfies $2.28 \leq \beta \leq 4.47$, but α is defined differently as the value such that $a/d_- = \lambda_0(\alpha)$. If $6.90 < a/d_-$, α is undefined and β is now redefined as the value such that $a/d_- = \lambda_0(\beta)$, so that $\beta > 4.47$. In the last case the redefinitions have the effect of replacing α by β, which facilitates a succinct statement of Theorem 2(iii) below.

These definitions of α and β can be expressed equivalently as locating intersections of the functions $\lambda_0(F_-)$, $\lambda_3(F_-)$ and $\lambda_4(F_-)$, using $\mu(\lambda_0) = 0$, (20), (22) and (23), as follows. α locates the intersection defined by

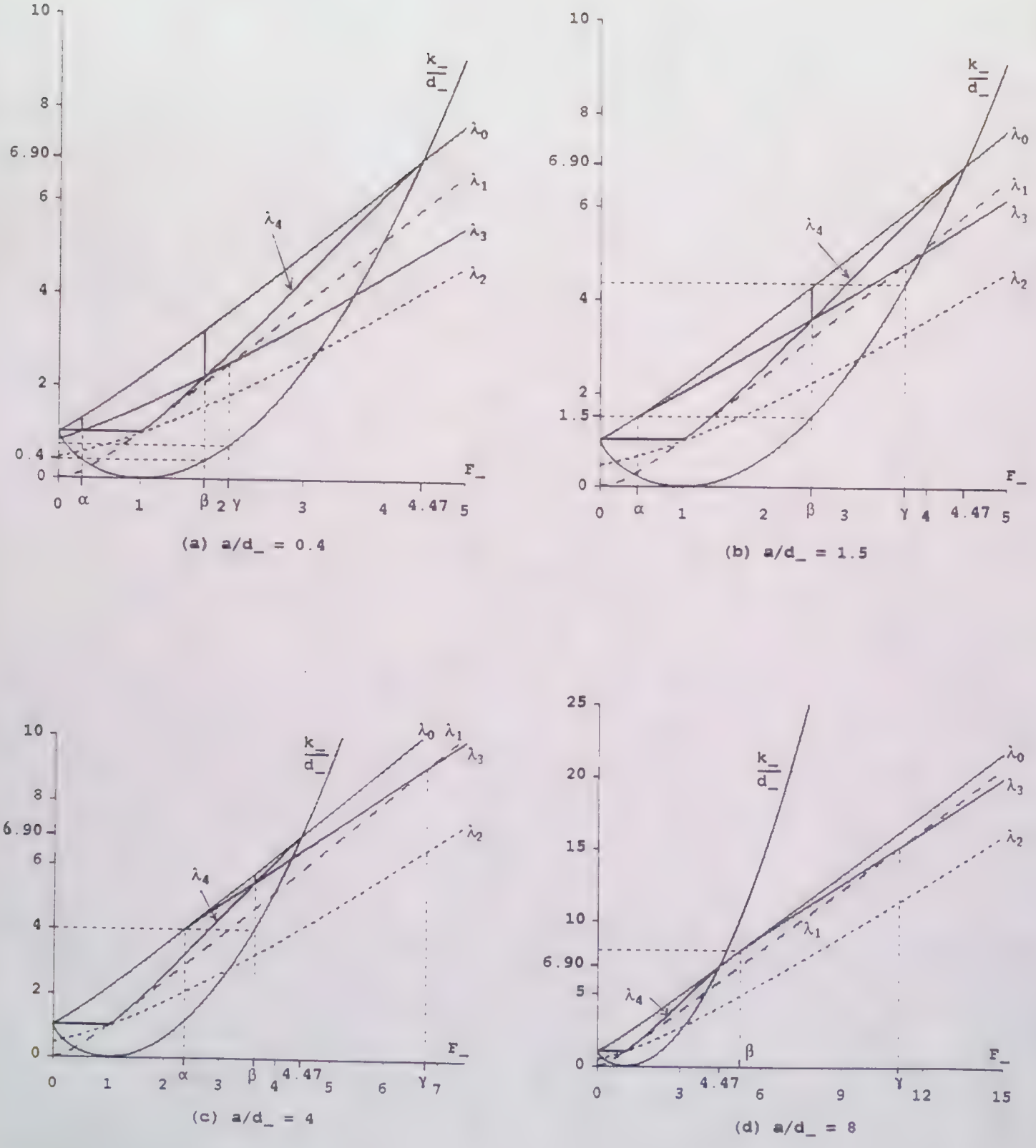

Figure 4. Functions of F_ deciding bore strength ranges.

$$\lambda_3(\alpha) = \begin{cases} 1 & \text{if } \begin{cases} 0 \le a/d_- \le 1 \\ 1 \le a/d_- \le 6.90 \,. \end{cases} \\ \lambda_0(\alpha) \end{cases} \tag{24}$$

β locates the intersection defined by

$$\lambda_3(\beta) = \begin{cases} \lambda_4(\beta) & \text{if } \begin{cases} 0 \le a/d_- \le 6.90 \\ a/d_- > 6.90 \,. \end{cases} \\ \lambda_0(\beta) \end{cases} \tag{25}$$

For all $a/d_- > 0$, γ denotes the unique intersection of $\lambda_3(F_-)$ and $\lambda_1(F_-)$, so that

$$\lambda_3(\gamma) = \lambda_1(\gamma) \,, \tag{26}$$

and $\gamma > \beta$ as Figure 4 shows. If $a = 0$, $\gamma = \beta = 1$.

Summarizing thus far, the foregoing paragraphs define the functions $\lambda_0(F_-)$, $\lambda_1(F_-)$, $\lambda_2(F_-)$, $\lambda_3(F_-, a/d_-)$, $\lambda_4(F_-)$ and $k_-(F_-)$, only one of which depends on a/d_- as well as F_-. In terms of these functions, shown in Figure 4, we are in a position to establish the main results about bores of type (16), which we express in the following theorems. (In Broad, Porter and Sewell (1992b) λ_+, λ_2 λ_3 were used to denote the present λ_2, λ_3, λ_4 respectively).

Theorem 1

(i) The outgoing flow from any such bore must be subcritical ($F_+ < 1$), for every type of incoming flow whether it be subcritical or supercritical, and whether the inflow would be free, bifurcating or blocked.

(ii) No such bore can exist if

$$\frac{a}{d_-} \ge \lambda_0 \tag{27}$$

because this implies that the outgoing flow would be blocked.

Proof

(i) From (12) the Froude number $F_+ = u_+ / (gd_+)^{\frac{1}{2}}$ on the right of the bore can be written $F_+ = \mu / \lambda^{3/2}$. With (14) this defines a function $F_+(\lambda)$ such that $F_+(\lambda_2) = 1$ for each F_-. Allowing F_- to vary then defines the function $\lambda_2(F_-)$, which increases with F_- as shown in Figure 4, and $\lambda_2(1) = 1$. If $F_- < 1$, then $\lambda_1 < \lambda_m < \lambda_2 < 1$, and if $F_- > 1$ then $1 < \lambda_m < \lambda_2 < \lambda_1$, as Figure 3 illustrates. Therefore, for every $F_- > 0$, λ_2 is strictly to the left of the sufficient domain of physical interest established after (19), so that $\mu^2 < \lambda^3$. In other words, any outgoing flow from a bore must be subcritical.

(ii) Since $k_+(\lambda)$ is monotonically increasing in $\lambda_2 \le \lambda < \lambda_0$, which includes the domain of physical interest, $k_+(\lambda) < \lambda_0 d_-$ there. Then (27) implies $a > k_+(\lambda)$, which violates the last condition in (16) requiring that the outgoing flow should not be blocked.

□

Theorem 2

(i) If the incoming flow would be blocked, then for each value of a/d_- satisfying

$$\frac{k_-}{d_-} < \frac{a}{d_-} < \lambda_0 \tag{28}$$

a bore satisfying (16) can exist only for incoming flows in the range

$$\alpha < F_- < \beta \le 4.47 \tag{29}$$

illustrated in Figure 4(a), (b) and (c). The strength λ of such a bore must lie in the range

$$\lambda_3 \le \lambda < \lambda_0 \le 6.90 . \tag{30}$$

The outgoing flow from every such bore relieves the blocking, and none of these bores can be stationary. The outflow from the weakest bore with strength λ_3

becomes critical when it reaches the apex, and permits a bifurcation there. Stronger bores induce a free flow over the apex. Blocking cannot be relieved by any such bore if $F_- \geq 4.47$, and correspondingly, no such bore which relieves blocking can have strength greater than 6.90. This is the sense in which an inflow with $F_- \geq 4.47$ can be called *hypercritical.*

(ii) If the incoming flow would bifurcate, so that

$$k_- = a < \lambda_0 d_- , \tag{31}$$

a bore satisfying (16) can exist only for the particular incoming flows

$$F_- = \alpha < 1 , \quad \text{and} \quad F_- = \beta \quad \text{with} \quad 1 < \beta < 2.28, \quad \text{if} \quad 0 < a < d_- ,$$

$$F_- = \beta \quad \text{with} \quad 2.28 \leq \beta < 4.47 \quad \text{if} \quad d_- \leq a < 6.90 d_- . \tag{32}$$

The strength λ of such bores must lie within the ranges

$$1 < \lambda < \lambda_0 \quad \text{if} \quad F_- = \alpha , \qquad \lambda_3 \leq \lambda < \lambda_0 \quad \text{if} \quad F_- = \beta . \tag{33}$$

When $F_- = \beta$ the outflow from the weakest bore bifurcates at the apex, and the free surface height there is less than that which the bifurcation would have had if the bore had not intervened. None of these bores can be stationary.

(iii) If the incoming flow would be free, we have

$$a < k_- \leq \lambda_0 d_- \quad \text{if} \quad F_- \leq 4.47 \tag{34}$$

or

$$a < \lambda_0 d_- \leq k_- \quad \text{if} \quad F_- \geq 4.47 . \tag{35}$$

In these cases a bore satisfying (16) can exist only for incoming flows in the ranges

$$0 < F_- < \alpha \quad \text{if} \quad a < d_- , \quad \beta < F_- . \tag{36}$$

The strength λ of such bores must lie within the ranges

$$1 < \lambda < \lambda_0 \quad \text{if} \quad 0 < F_- < \alpha \ \text{with} \ a < d_-, \tag{37}$$

$$\lambda_3 \leq \lambda < \lambda_0 \quad \text{if} \quad \beta < F_- \leq \gamma, \tag{38}$$

$$\lambda_1 \leq \lambda < \lambda_0 \quad \text{if} \quad \gamma \leq F_-. \tag{39}$$

The outflow from the weakest bore in (38) bifurcates at the apex. None of the bores in (37) or (38) are stationary, but the weakest bore in (39) is stationary.

Proof

(i) Apex heights satisfying (28) ensure that the inflow would be blocked ($k_- < a$), and therefore that the curve $k_-(F_-)$ shown in Figure 4 must be below the height a. This means that $F_- < \beta \leq 4.47$ for all a such that $0 < a/d_- \leq 6.90$. It also means that $F_- > \alpha$ if $0 < a/d_- \leq 1$. For $1 \leq a/d_- \leq 6.90$, it is $a/d_- < \lambda_0$ in (28) which implies $F_- > \alpha$. This establishes (29) in terms of the definitions of α and β given after (23). The hypothesis $a/d_- < \lambda_0$ also permits some $\lambda \geq \lambda_3$ such that $k_+(\lambda) \geq a$, so that certain bores are possible whose outflow is not blocked. Examples of such a/d_- are illustrated in Figure 3, namely $a/d_- = 0.7$, 2.8 and 5 for $F_- = 0.2, 2.5$ and 6 respectively. These illustrate how λ_3 is defined by $k_+(\lambda_3) = a$, so that $a \leq k_+ < \lambda_0 d_-$ specifies the range (30), by the monotonicity of $k_+(\lambda)$ and $\mu(\lambda)$. The range (29) is then alternatively implied by the definitions (24) and (25) of α and β as intersections involving $\lambda_3(F_-)$.

The property $k_+(\lambda_3) = a$ implies, by our analysis in §2, that there will be a bifurcation at the apex, with $F = 1$ there. Stronger bores with $\lambda_3 < \lambda < \lambda_0$ therefore imply a free flow. Examples are shown in Figure 5. The range (28) vanishes at $F_- = 4.47$ because this is the intersection $k_-(F_-) = d_-\lambda_0(F_-)$ shown in Figure 4, and $\lambda_0(4.47) = 6.90$. This proves that blocking cannot be relieved if $F_- \geq 4.47$.

We can see from the illustrations in Figure 4(a), (b) and (c) that $\lambda_3 > \lambda_1$ in (29), because $\gamma > \beta$ when $a > 0$. This proves that no bore which relieves blocking can be stationary, because $C(\lambda_1) = 0$. Instead, the weakest such bore has speed

$$-C = \left[\left[\tfrac{1}{2}\lambda_3(\lambda_3+1)\right]^{\frac{1}{2}} - F_-\right](gd_-)^{\frac{1}{2}} > 0 \qquad (40)$$

from (15).

The following alternative argument is worth noticing. A stationary bore $(C = 0)$ would satisfy $[Q] = 0$ from $(8)_1$ and $[e] < 0$ from $(11)_2$, and therefore $[k] < 0$ from (4), i.e. $k_+ < k_-$. But this would contradict joint hypotheses $a \le k_+$ and $k_- \le a$. This proves that blocked or bifurcating inflow and a free or bifurcating outflow cannot coexist with a stationary bore.

(ii) The values of F_- at which $a = k_-$ are, by definition, those in (32), as illustrated in Figure 4(a), (b) and (c). The strength ranges (33) follow, for example by examining Figure 4. When $F_- = \alpha$ the weakest bore is only nascent $(\lambda \longrightarrow 1)$, but when $F_- = \beta$ the weakest bore has strength λ_3, and since $k_+(\lambda_3) = a$, this implies a bifurcation when the outflow reaches the apex. None of these bores are stationary because $\gamma > \beta > \alpha$.

The general formulae at the beginning of §2 allow the local free surface height to be written as

$$s = \frac{e - gb}{g(1 + \frac{1}{2}F^2)} + b = \frac{(Q^2/g)^{1/3}(3G/2)}{1 + \frac{1}{2}F^2} + b \qquad (41)$$

in terms of F and the constants of the motion. When there is a bifurcation point over the apex $F = 1$ and $b = a$, so the free surface height there is $\frac{2e}{3g} + \frac{1}{3}a = (Q^2/g)^{1/3} + a$. From $(8)_1$, $(10)_2$ and (16) $[Q] = C[d] < 0$ at the bore, so that $Q_+ < Q_-$. This proves that, when $F_- = \beta$, the free surface height of the bifurcation over the apex implied by $k_- = a$ is decreased when the weakest

bore intervenes, implying $k_+ = a$. A diagram illustrating this decrease over a symmetric cubic mountain, and thus showing how two different bifurcation points over the apex are available to the incoming flow, is given by Broad, Porter and Sewell (1992b, 1994). Here we have been more specific than previously about the particular incoming flows (32) which permit bores (33) to intervene in an already bifurcating flow.

(iii) Apex heights satisfying $a < k_-$ ensure that the inflow would be free, and also that the curve $k_-(F_-)$ shown in Figure 4 must be above the height a. This means that $F_- > \beta$ in the case of (34) as Figure 4(a), (b) and (c) illustrates, and that $0 < F_- < \alpha$ if $a < d_-$ as Figure 4(a) illustrates. In the case of (35) it is the curve $\lambda_0(F_-)$ which must be above a/d_-, which requires the redefined β in $(25)_2$ to be such that $F_- > \beta$. This proves (36).

The ranges (37) – (39) then follow, as the illustrations in Figure 4 make clear. When $F_- > 1$ with $a < k_-$ we see that $\lambda_3 < \lambda_4$, and the least admissible strength is either λ_3 (for which the outflow bifurcates at the apex) if $F_- < \gamma$, or λ_1 (for which the bore is stationary) if $F_- \geq \gamma$.

Previous arguments can be repeated to establish the bifurcation and non–stationary properties. □

Evidently if the inflow is fast enough $(F_- \geq \gamma)$ the weakest bore satisfying (16) is always stationary when (35) applies. This gives a situation in which *two* truly *steady* flows are possible, namely one free flow without the bore and one flow with the bore. The outflow from the latter is free if $F_- > \gamma$, and bifurcates over the apex if $F_- = \gamma$. By contrast, a flow with a moving bore is only pseudo–steady.

A diagram showing the free surface over a symmetric cubic mountain for a free incoming flow having $F_- = 1.73$, together with an intervening bore of strength $\lambda_3 = 2.06$

from which the outflow bifurcates over the apex, is given by Broad, Porter and Sewell (1992b, 1994). This illustrates (38).

Theorem 3

Among the bores (16) whose strength satisfies (30), (33), (37), (38) or (39), the weakest one involves the least energy dissipation $-E$ and the least $[e]$.

Proof

The minimum energy dissipation property follows from the monotonic character of (13) in every case.

Another non–dimensional variable ν with values defined by

$$\nu gd_- = \tfrac{1}{2} u_+^{\,2} + gd_+ , \quad \text{so that} \quad \nu(\lambda) = \tfrac{1}{2}\left[\frac{\mu}{\lambda}\right]^2 + \lambda , \tag{42}$$

can be added to the list (12). It can be shown that $\nu(\lambda)$ is an increasing function, and this establishes the minimizing property of $[e]$ at the weakest bore, because $e_+ = \nu gd_-$ where $b = 0$. □

It follows from Theorem 3 that, if minimum energy dissipation is adopted as a hypothesis, it selects the weakest bores from the admissible ones determined in Theorem 2. The outflow from such weakest ones has a bifurcation at the apex in the case of (30), $(33)_2$ and (38), but is a free flow in the case of $(33)_1$, (37) and (39).

The monotonicity of $-E$ also indicates that if $C > 0$ is permitted when $F_- > \gamma$, less energy would be dissipated than if $C = 0$. In other words, weaker bores than $(39)_1$, with strength in the range $\lambda_3 \le \lambda < \lambda_1$, would dissipate less energy if they were allowed to run downstream (instead of being stationary) while facing upstream. This is in the case when the incoming flow would be free otherwise.

We are not aware whether hypercritical inflows have been observed in nature. Clearly they would be harder to achieve in certain laboratory experiments than those commonly quoted. As we have seen, however, their mathematical properties have some novel features.

Next we derive some relations between the *pairs* of steady continuous flows which can have the *same* given values of $Q > 0$ and e in (3) at a location with bed height b (perhaps $b = 0$ in particular). Such values specify a single given value of G in $(2)_1$, and we have seen that whenever such $G > 1$, Figure 1 shows that there are *two* possible values of F. We shall find it convenient to write them as F and F^*. That is, one flow of the pair is "unstarred", and the star denotes "the other flow". One is subcritical and the other is supercritical, but we do not need to say which is which.

Theorem 4

(i) The speed and depth of the unstarred and starred flows in a pair are related by

$$\frac{d^*}{d} = \frac{1}{4}F\left[(8+F^2)^{\frac{1}{2}} + F\right] \quad , \quad \frac{u^*}{u} = \frac{1}{2F}\left[(8+F^2)^{\frac{1}{2}} - F\right] , \tag{43}$$

$$\frac{8}{F^*} = F^{\frac{1}{2}}\left[(8+F^2)^{\frac{1}{2}} + F\right]^{3/2} . \tag{44}$$

(ii) The pairs immediately on either side of a bore satisfying (16) are related as follows. All the bores with $F_- < 1$ which are described by Theorem 2 have

$$F_+ < F_- < 1 < F_-^* < F_+^* \tag{45}$$

and

$$d_+^* d_-^* < d_+^* d_- < d_+ d_-^* < d_+ d_- . \tag{46}$$

All the bores with $F_- > 1$ which are described by Theorem 2(i) and (ii) have

$$F_+ < F_-^* < 1 < F_- < F_+^* \tag{47}$$

and

$$d_+^* d_- < d_+^* d_-^* < d_+ d_- < d_+ d_-^* \ . \tag{48}$$

All the bores with $F_- > \beta$ which are described by Theorem 2(iii) have the properties (47) and (48) when $G_+ > G_-$. For these bores (38) and (39), however, it may happen that either $G_+ = G_-$ which implies

$$F_+ = F_-^* < 1 < F_- = F_+^* \tag{49}$$

and

$$d_+^* d_- < d_+^* d_-^* = d_+ d_- < d_+ d_-^* \ , \tag{50}$$

or that $G_+ < G_-$ which implies

$$F_-^* < F_+ < 1 < F_+^* < F_- \tag{51}$$

and

$$d_+^* d_- < d_+ d_- < d_+^* d_-^* < d_+ d_-^* \ . \tag{52}$$

Proof

(i) From the definitions above and at the beginning of §2,

$$e - gb = \tfrac{1}{2} u^2 + gd = \tfrac{1}{2} u^{*2} + gd^* \ , \quad Q = ud = u^* d^* \ . \tag{53}$$

Eliminating u from the first of each of these equations gives

$$\frac{e - gb}{gd} = \frac{Q^2}{2gd^3} + 1 \ ,$$

and a similar equation for d^* by eliminating u^*. Therefore both 1 and d^*/d are roots ξ of

$$\frac{(e - gb)\xi^2}{gd} = \frac{Q^2}{2gd^3} + \xi^3 \ .$$

With (53) this can also be written as

$$\xi^3 - (\tfrac{1}{2}F^2 + 1)\xi^2 + \tfrac{1}{2}F^2 = 0 .$$

This equation has roots 1 and $\frac{1}{4}F\left[F \pm (8+F^2)^{\frac{1}{2}}\right]$. This proves $(43)_1$, and $(43)_2$ is its reciprocal, by $(53)_2$. Combining (43) gives (44).

(ii) The function $F_+(\lambda) = \mu(\lambda)/\lambda^{3/2}$ defined from (12) is a monotonically decreasing function of λ such that $F_+(1) = F_-$. Therefore $F_+ < F_-$ for every bore except the nascent one.

Hence if $F_- < 1$, the corresponding ordinates on Figure 1 must have the property $G_+ > G_-$, and horizontal lines through these values meet the convex curve a second time to define the starred flows such that $F_+^* > F_-^* > 1$. This proves (45). Then (46) follows from the monotonically increasing nature of the function f(F) (say) on the right of $(43)_1$, applied to $f(F_+) < f(F_-)$.

If $F_- > 1$, we know that $F_+ < 1$ from Theorem 1(i). Next we need to note the general formula that

$$g(k-b) = \tfrac{3}{2}(gQ)^{2/3}(G-1) \qquad (54)$$

from (2) and (4), so that since $Q_- \neq 0$ from $(16)_1$,

$$\frac{G_- - 1}{G_+ - 1} = \frac{k_-}{k_+}\left[\frac{Q_+}{Q_-}\right]^{2/3} . \qquad (55)$$

From $(8)_1$ we have $Q_+ = Q_- + (\lambda - 1)Cd_-$, and using (14), (15) and (16) allows (55) to be expressed as a function of λ and F_-.

The family of bores (30) in the range $1 < F_- < \beta$ belonging to (29) has $C < 0$ and $k_+ \geq a > k_-$. The bores $(33)_2$ have $C < 0$ and $k_+ \geq a = k_-$. In each case $G_- < G_+$ from (55), and the horizontal lines through these unstarred points on

Figure 1 show that the starred points satisfy (47). Then (48) follows from the property $f(F_+) < f(F_-^*)$ of $(43)_1$.

If $\beta < F_- < 4.47$ the families (38) and (39) each contain a bore of strength $\lambda_4 > \lambda_1$ for which $k_+ = k_-$ and $Q_+ < Q_-$, so that $G_+ > G_-$ from (55). Therefore (47) applies to such a bore.

If $\gamma \leq F_-$ the weakest member of the family (39) has $Q_+ = Q_-$, and if $\gamma < 4.47$ also, $k_+(\lambda_1) < k_+(\lambda_4) = k_-$, so that $G_+ < G_-$ for such a bore (again from (55), to which (51) then applies.

By continuity, when $\gamma \leq F_- < 4.47$, there will be a member of the family (39) such that $G_+ = G_-$, to which (49) therefore applies.

□

6. Examples of Bores which relieve Blocking

Examples of bores which relieve blocking and have properties established in Theorems 1, 2(i), 3 and 4 are displayed in Figure 5. Symmetric parabolic and quartic obstacles (5) are chosen, namely $b(x) = 1.2(1-(x/\ell)^2)$ and $b(x) = 1.2(1-(x/\ell)^4)$ for $|x| \leq \ell$, with $b(x) = 0$ elsewhere. The free surface height functions $s(x)$ are shown, for the pair of incoming flows which, on the left of the bore, have the same values $Q = 9$, $e = 7.5$, $g = 1$. These are also the constants chosen in the paragraph after (5). Since $k_- = 1.01$ from (4), and $a = 1.2$, each incoming flow is blocked and could only progress as far as the end of the curve shown by short dashes (after which the curve must turn back into its paired version, like the blocked $u(x)$ functions in Figure 2). The block can be overcome by a bore travelling to the left over the flat plain, and we show two such bores in each part of Figure 5.

Each full line shows a bore which overcomes the block with minimum energy dissipation $-E(\lambda_3)$ in (13). When the outgoing flow from the bore reaches the apex it bifurcates according to Theorem 2(i), abruptly so over the parabola and smoothly so over the quartic. For the subcritical incoming flow, solving $k_+(\lambda_3) = 1.2$ delivers the

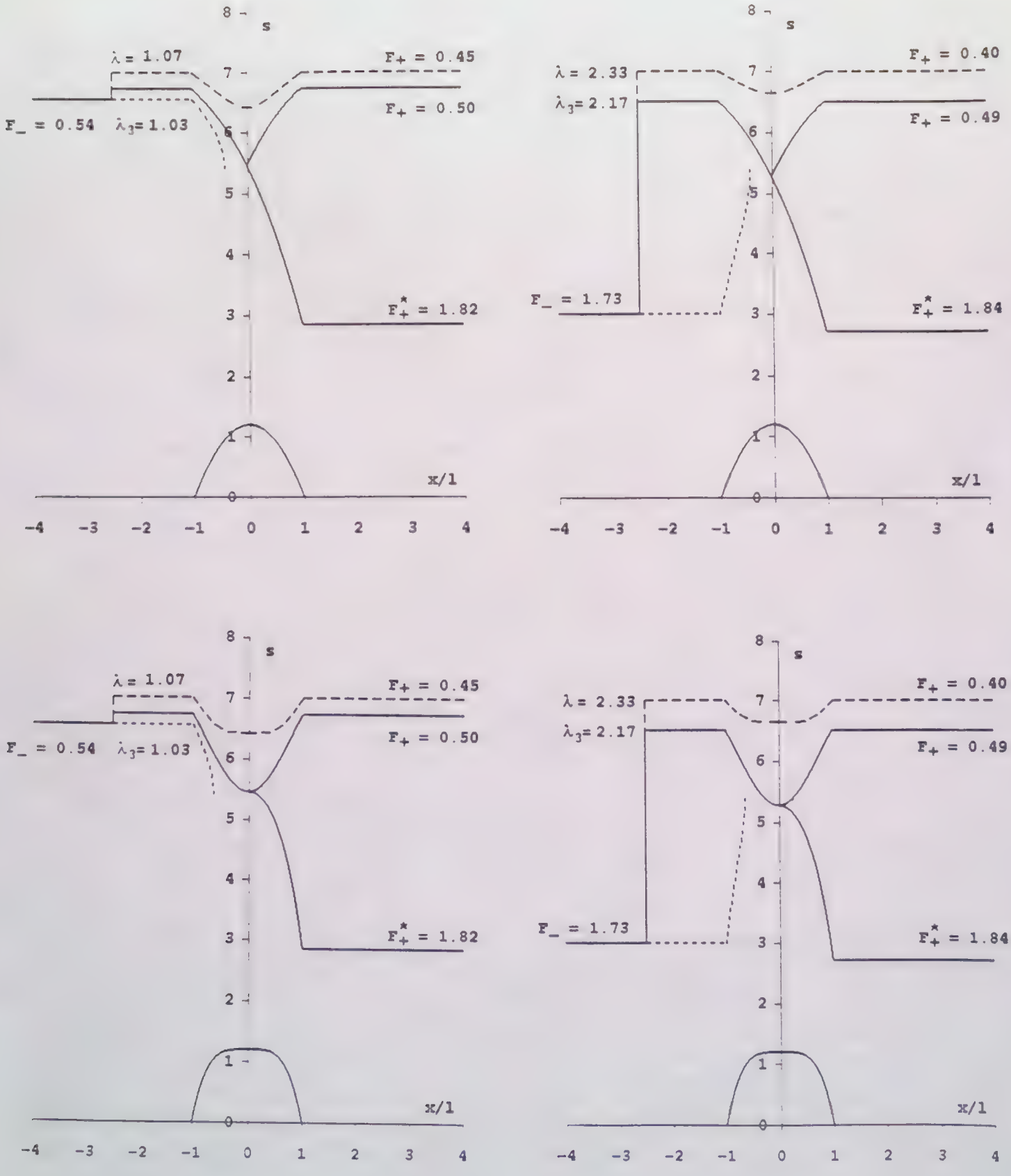

Figure 5. Free surface profiles illustrating relief of blocking.

minimum bore strength $\lambda_3 = 1.03$, and the immediately outgoing flow has $F_+ = 0.50$, $u_+ = 1.30$, $d_+ = 6.73$. These values are recoverable, after the bifurcation, downstream on the flat plain to the right of the mountain, as shown. The bifurcation also makes available a supercritical flow to the right of the apex, and when this reaches the flat plain it has $F_+^* = 1.82$, $u_+^* = 3.08$, $d_+^* = 2.86$ as shown. The supercritical incoming flow has minimum bore strength $\lambda_3 = 2.17$, and the immediately outgoing flow has $F_+ = 0.49$, $u_+ = 1.26$, $d_+ = 6.52$. These values are also recoverable, after the bifurcation, downstream of the mountain, as shown. The bifurcation also makes available a supercritical flow to the right of the apex, and when this reaches the flat plain it has the values $F_+^* = 1.84$, $u_+^* = 3.03$, $d_+^* = 2.72$ shown.

The long dashes in Figure 5 illustrate how a bifurcation in the free surface is avoided if the bore dissipates more energy than the minimum value $-E(\lambda_3)$, with a bore strength λ lying strictly within the range (30). For the subcritical incoming flow we have chosen $\lambda = 1.07 > 1.03$ with $k_+ = 1.52 > 1.2$, so that on the flat plain $F_+ = 0.45$, $u_+ = 1.2$, $d_+ = 7$. For the supercritical incoming flow we have chosen $\lambda = 2.33 > 2.17$ with $k_+ = 1.88 > 1.2$, so that on the flat plain $F_+ = 0.40$, $u_+ = 1.05$, $d_+ = 7$.

The bores in Figure 5 are shown when they are in the same place, for convenience, but they will be moving at different speeds to the left as given by (40) and (15). The speeds $-C(\lambda_3)$ of the weakest bore which unblocks the subcritical and supercritical incoming flows are 1.24 and 0.22 respectively. The speeds of the stronger bore, which dissipates more energy, are 1.32 and 0.42 respectively. Bores which unblock the subcritical flow are evidently much faster than those which unblock the supercritical flow.

7. Summary of Solutions

In §3 we discuss continuous steady flows in the presence of an obstacle having apex height a. When the incoming $k > a$, the flow passes freely over the obstacle. When $k = a$, the fluid surface and the velocity each exhibit a bifurcation over the apex. For a family (5) of monotonic mountains we show, in Figure 2, how the local features of this

bifurcation are strongly dependent on the local shape of the mountain profile. In particular, the bifurcation is usually smooth, which seems not to have been pointed out before. There is an exceptional case in which the bifurcation is abrupt, over the parabolic mountain, but only this last case has been reported in the literature, as far as we are aware. When $k < a$, the flow is blocked and cannot surmount the obstacle unless an upstream bore intervenes, which makes the flow discontinuous.

Blocking can be relieved by a bore moving upstream away from the mountain. This creates a discontinuous pseudo–steady flow which lifts the fluid so that it can flow over the mountain, as illustrated in Figure 5. Bores in the same family (16) can also exist as alternatives to an incoming flow which would be already free, or at least bifurcate over the apex, even though such bores are not then needed to relieve blocking. The main properties of all these bores are described in Theorems 1, 2 and 3. Theorem 4 describes *pairs* of steady continuous flows which can co–exist, in particular on the two sides of a bore, including those in Figure 5.

Theorems 1, 2 and 3 include, for the first time, complete information about the strength λ of such bores of type (16). This fact allows us to summarize our results unambiguously in a three dimensional space spanned by $F_- \geq 0$, $a/d_- \geq 0$ and $\lambda \geq 1$. For clarity we show first, in Figure 6, the single valued surface in this space which describes the weakest of such bores. These are the bores which, according to Theorem 3, dissipate the least energy.

If one chooses to adopt that physical hypothesis, then the only bores (16) which remain in Theorem 2 are those with strength λ_3 in (30), $(33)_2$ and (38), and those with strength λ_1 in (39). The weakest bores in $(33)_1$ and $(37)_1$ are only nascent ones, which will not actually be noticed. The continuous surface shown in Figure 6 therefore consists of two contiguous smooth parts ABCE and CED, which join at a crease CE across which the surface has a discontinuity of gradient. The part ABCE has equation (20), which is an implicit definition of a function

$$\lambda = \lambda_3(F_-, a/d_-) . \tag{56}$$

We recall that λ_3 is defined by the condition $k_+(\lambda_3) = a$ that the outflow from the bore will bifurcate when it reaches the apex. The part CED is a cylinder, parallel to the a/d_- axis, with equation

$$\lambda = \lambda_1(F_-) \tag{57}$$

where the function on the right is defined by (19), and a bore with strength λ_1 is stationary.

BCD is the intercept of the composite surface with the vertical plane $F_- = 6$, and for $F_- > 6$ our theory shows that there are no additional features. The surface ABCE has three other boundaries. It actually meets the plane $\lambda = 1$ in the curve AE, whose equation is

$$\frac{a}{d_-} = \frac{1}{2}F_-^2 + 1 - \frac{3}{2}F_-^{3/2} \tag{58}$$

from (20) with $\lambda_3 = 1$ there. The surface otherwise lies in the half space $\lambda > 1$, representing the condition that the bore must face upstream. The coordinates of A are $F_- = 0$, $a/d_- = \lambda = 1$ and those of E are $a/d_- = 0$, $F_- = \lambda = 1$.

The space curve AB is

$$\lambda = \lambda_0(F_-) = a/d_- . \tag{59}$$

This is the common boundary of the conditions $u_+ > 0$, that the bore cannot stop or reverse the flow, and $k_+ \geq a$, that the outflow from the bore shall not be blocked. The curve AB terminates the surface (56) in that direction; any point on AB represents a bore moving away from the mountain at a speed $((\lambda_0 + 1)/2\lambda_0)^{\frac{1}{2}}$ which is just enough to reduce the outflow from it to what is required to maintain a reservoir of still water ($u_+ = 0$), between the bore and the apex, whose depth is the height of the mountain ($k_+ = a$).

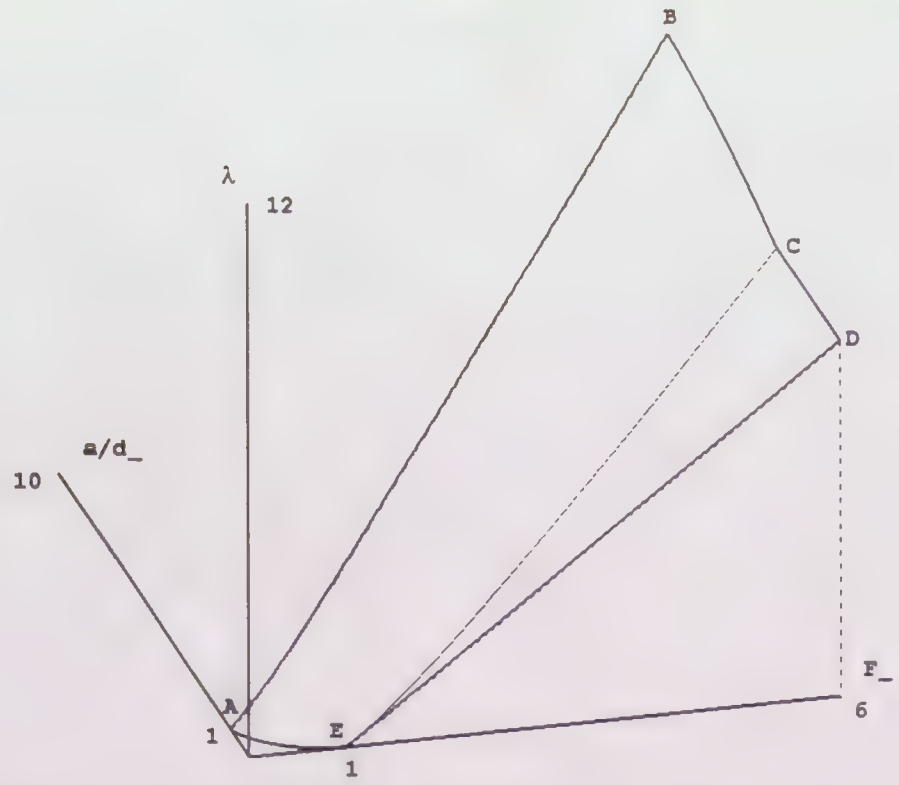

Figure 6. Weakest bore strength surface $\lambda = \lambda(F_\,,\, a/d_)$, representing bores which dissipate least energy.

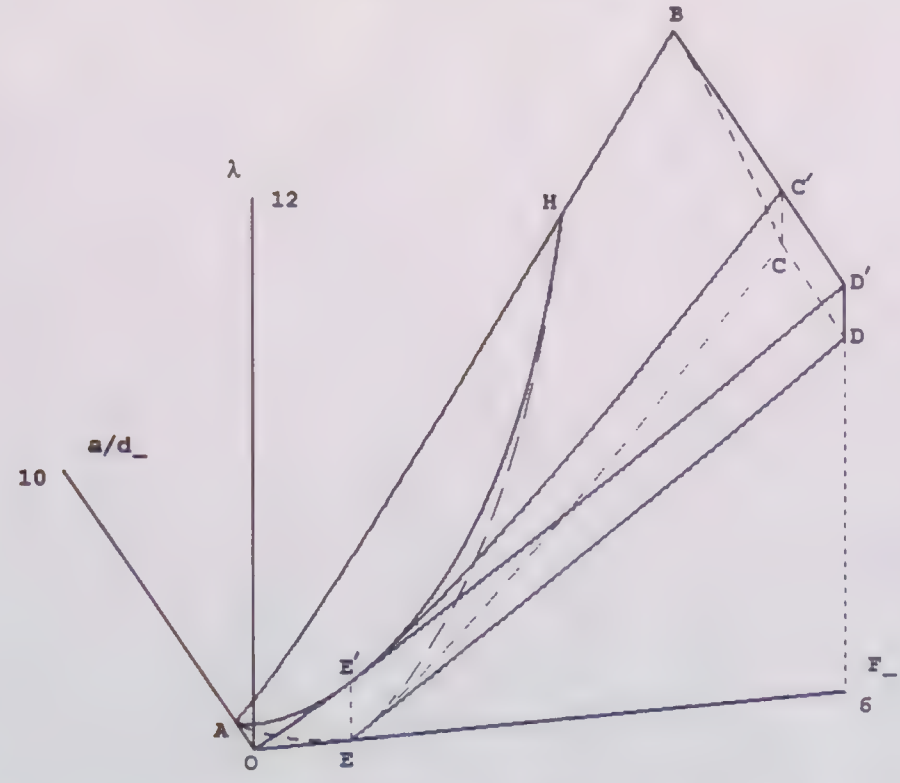

Figure 7. Available bore strengths (30), (33), (37), (38), (39) if more than the least energy can be dissipated.

The space curve CE is

$$\lambda = \lambda_1(F_-) = \lambda_3(F_-, a/d_-) \tag{60}$$

in terms of (56) and (57). This represents the weakest bore in both (38) and (39); any point on CE therefore represents a bore which is stationary and with an outflow which bifurcates at the apex, and for which $F_- = \gamma$ as described by (26). We could write (26) more explicitly as $\lambda_3(\gamma, a/d_-) = \lambda_1(\gamma)$ to emphasize that γ depends on a/d_-.

The cylinder CED has one other boundary ED, where it meets the plane $a/d_- = 0$ corresponding to the case of no obstacle. Any point on the interior of CED represents a stationary bore (in an incoming flow which would otherwise be free anyway) which minimizes the energy dissipation among other bores (16) which could move away from the obstacle. Such a stationary bore has an outflow which will pass freely over the obstacle, because such $\lambda_1 > \lambda_3$, as Figure 4(d) illustrates for $F_- > \gamma$. Bores which move towards the obstacle would dissipate even less energy than the stationary one, because the extension of ABCE passes below ECD, but they would run up against the obstacle after a finite time, which is why we excluded them at the beginning of §5.

Any point on the interior of ABCE represents a bore moving away from the obstacle which minimizes the energy dissipation among other such bores (16). The precise location of that point on ABCE will determine whether the flow in which the bore can exist would be otherwise blocked (as in (30)), bifurcating (as in $(33)_2$) or free (as in (38)). We omit the latter information from Figure 6, but introduce it into Figure 7.

The condition $\lambda = \lambda_0(F_-)$ defined by (18) represents zero outflow $u_+ = 0$ from a bore, and in Figure 7 it is shown as a part AHBC′D′E′OA of a cylinder parallel to the a/d_- axis, meeting the plane $a/d_- = 0$ in the curve D′E′O. The possible bore strengths calculated in (30), (33), (37), (38) and (39) lie between that surface AHBC′D′E′OA and the lower surface AHBCDEOA. The latter is already shown in Figure 6, and repeated in Figure 7. Points C′, D′ and E′ are vertically above C, D and E respectively. O is the point $F_- = a/d_- = 0$, $\lambda = 1$.

The surface CEE′C′C is part of a vertical cylinder, parallel to the λ axis, with equation $(60)_2$. Each point within the three dimensional region CEE′C′D′DE represents a bore (39) which can exist as an alternative to a supercritical incoming free flow.

The surface AE′HEA is part of another vertical cylinder, also parallel to the λ axis, with equation (58). Each point within the three dimensional region bounded by AE′HEA and the two surfaces AHE′A and AHEA, which is shaped like the segment of an orange, represents a bore (30) which can relieve blocking, in circumstances where no free flow is possible. The point H has coordinates $F_- = 4.47$, $a/d_- = \lambda = 6.90$.

Each point within the three dimensional region bounded by the part AE′EA of the vertical cylinder (58), the part AE′OA of the cylinder $\lambda = \lambda_0(F_-)$, the part of AEOA of the base plane $\lambda = 1$, and the part OE′EO of the plane $a/d_- = 0$, represents a bore (37) which can exist as an alternative to a subcritical incoming free flow.

Each point on the part AE′EA of the vertical cylinder (58) represents a bore $(33)_1$ which can exist as an alternative to a subcritical incoming bifurcating flow.

Each point on the part HE′EH of the vertical cylinder (58) represents a bore $(33)_2$ which can exist as an alternative to a supercritical incoming bifurcating flow.

Each point within the three dimensional region bounded by the part HE′EH of the vertical cylinder (58), the part HE′C′BH of the cylinder $\lambda = \lambda_0(F_-)$, and the part HECBH of the surface (56), represents a bore (38) which can exist as an alternative to a supercritical incoming free flow.

Free flows with no bore have $\lambda = 1$, and can therefore be represented on the base plane $\lambda = 1$ of Figures 6 and 7. Therefore, we complete our three dimensional representation of the flows established in this paper by showing, in Figure 8, the free flows added to Figure 6, and the same could be done for Figure 7. Again, nothing significant is omitted by our restriction to $F_- \leq 6$ in Figure 8. It shows the curve AEJ, whose equation is (58) with $\lambda = 1$, and the lift of part of that curve to AEH on the surface AHBCEA. The curve AEJ divides the plane $\lambda = 1$ into three parts, representing

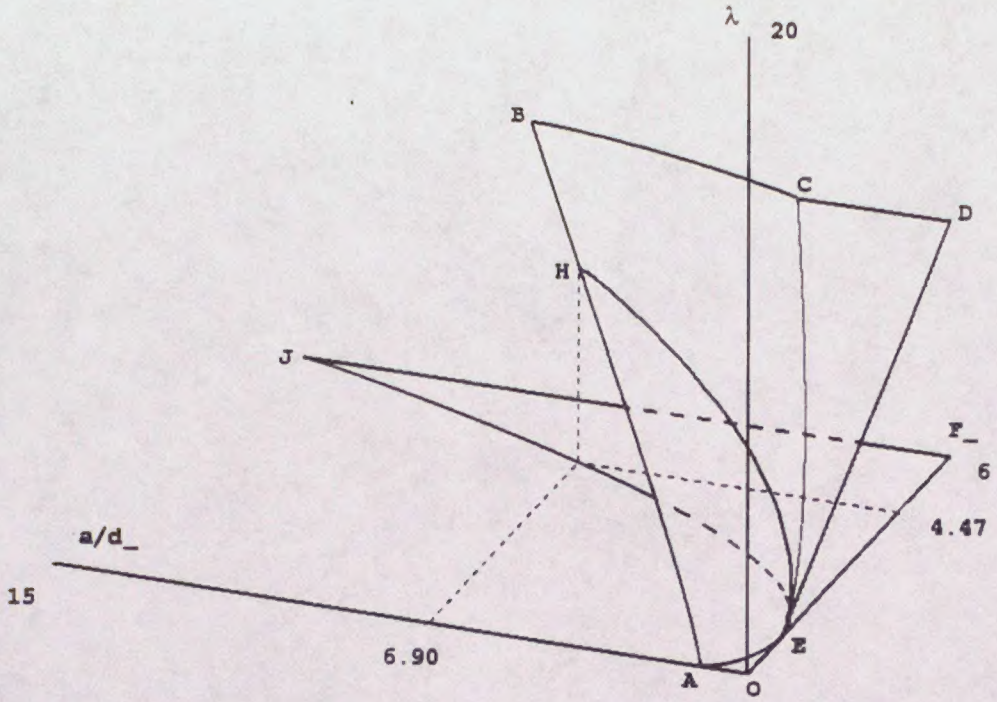

Figure 8. Free flows and weakest bores.

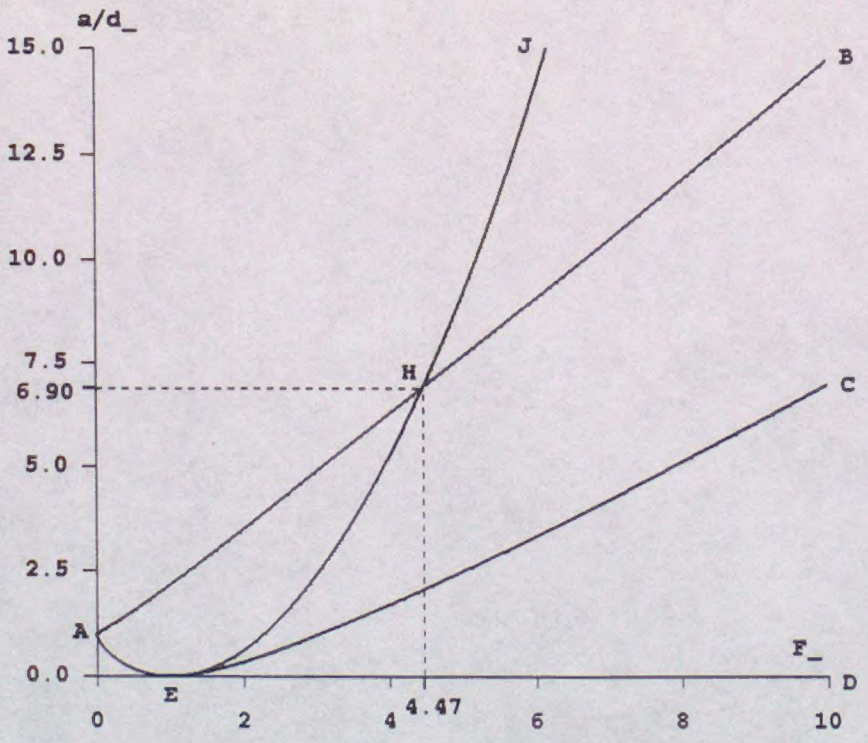

Figure 9. Plane classification diagram.

blocked flows (for a/d_- values greater than that in (58)) and free flows (for a/d_- values less than that in (58)). The free flows are subcritical in the sector AEO, and supercritical on the other side of E ($F_- = 1$ at E). The surface AEHA portrays those bore strengths which can relieve blocked flows and have minimum energy dissipation, and the remaining part EHBCDE portrays the other bores of Figure 6. The available bore strengths shown in Figure 7 can be added to Figure 8 to complete the three dimensional representation of our results.

8. Classification Diagram

We can now see from Figures 7 and 8 why a "classification diagram" in the F_-, a/d_- plane alone, which is how results in the previous literature have usually been summarized, is incomplete and ambiguous. The diagram given by Broad, Porter and Sewell (1992b, 1994), and shown in Figure 9, is essentially a projection of Figure 8 onto its base plane. The projection process removes the information about the bore strengths, which was not available in the previous literature anyway, and is obliged to present bores and certain free flows in the same two–dimensional regions when, in truth, they belong to different three dimensional regions, as Figure 8 makes clear.

Curve AEHJ has equation (58), and expresses the condition $k_- = a$ for the incoming flow to be a bifurcating flow. Points in Figure 9 which are in the F_-, a/d_- plane but which are above the curve AEHJ represent blocked flows; points which are below it represent free flows, either subcritical within AEO or supercritical within JHED.

Curve AHB has equation $a/d_- = \lambda_0(F_-)$ or

$$F_- = \left[1 - \frac{d_-}{a}\right]\left[\frac{a}{2d_-}\left[\frac{a}{d_-} + 1\right]\right]^{\frac{1}{2}}. \qquad (61)$$

Points within the region AHE represent bores which can relieve the blocking. No such bores exist within the region above AHJ. Bores cannot be an alternative to the supercritical free flow possible within JHB.

Curve EC has equation $(60)_2$ or

$$\frac{a}{d_-} = \frac{1 + (1 + 8F_-^2)^{3/2}}{16F_-^2} - \frac{3}{2}F_-^{2/3} - \frac{1}{4}. \qquad (62)$$

Bores moving away from the obstacle can be an alternative to the free supercritical flows possible within BHED. Such moving bores, or stationary ones if dissipation is minimized, can be an alternative to the free supercritical flows possible within CED.

Classification diagrams of this type which are given by other authors, including those referred to in §1, are confined to the small rectangle $0 \leq F_- \leq 2.5$, $0 \leq a/d_- \leq 1.25$. They therefore omit the intersection point H and the region JHB in particular.

References

Baines, P.G. (1984) *A unified description of two–layer flow over topography.* J. Fluid Mech. 146, 127–167.

Baines, P.G. (1987) *Upstream blocking and airflow over mountains.* Ann. Rev. Fluid Mech. 19, 75–97.

Baines, P.G. and Davies, P.A. (1980) *Laboratory studies of topographic effects in rotating and/or stratified fluids.* Orographic effects in planetary flows. WMO GARP Publ. Ser. 23, 233–299.

Broad, A.S., Porter, D. and Sewell, M.J. (1992 a) *A new approach to shallow flow over an obstacle I: General theory.* U.K. Meteorological Office Short Range Forecasting Division Scientific Paper No. 11, 54 pp.

Broad, A.S., Porter, D. and Sewell, M.J. (1992 b) *A new approach to shallow flow over an obstacle II: Plane flow over a monotonic mountain.* U.K. Meteorological Office Short Range Forecasting Division Scientific Paper No. 12, 58 pp.

Broad, A.S., Porter, D. and Sewell, M.J. (1994) *Shallow flow over general topography with applications to monotonic mountains.* Proceedings of the Fourth I.M.A. Conference on Stably Stratified Flows, edited by I. Castro and N. Rockliff, Oxford University Press, pp. 133–138.

Gill, A.E. (1977) *The hydraulics of rotating–channel flow.* J. Fluid. Mech. 80, 641–671.

Houghton, D.D. and Kasahara, A. (1968) *Nonlinear shallow fluid flow over an isolated ridge.* Comm. Pure and Appl. Math. 21, 1–23.

Lawrence, G.A. (1987) *Steady flow over an obstacle.* J. Hydraulic Engng. 113, 981–991.

Long, R.R. (1954) *Some aspects of the flow of stratified fluids II: Experiments with a two–fluid system.* Tellus 6, 97–115.

Long, R.R. (1970) *Blocking effects in flow over obstacles.* Tellus 22, 471–480.

Long, R.R. (1972) *Finite amplitude disturbances in the flow of inviscid rotating and stratified fluids over obstacles.* Ann. Rev. Fluid Mech. 4, 69–92.

Pratt, L.J. (1983) *A note on nonlinear flow over obstacles.* Geophys. Astrophys. Fluid Dyn. 24, 63–68.

Pratt, L.J. (1984) *On nonlinear flow with multiple obstructions.* J. Atmos. Sci. 41, 1214–1225.